# Flight Dynamics Modelling and Application to Satellite Deorbitation Strategy

Ulysse Marguery

KTH - Royal Institute of Technology
Aeronautical and Vehicle Engineering Department
SE - 100 44 Stockholm, Sweden

*e-mail: ulysse@kth.se*

January 5, 2011

**Abstract**

In this paper a study to determine the best strategic choice to deorbit satellites in case of system failures is conducted. An orbital mechanic analysis of the deorbitation is done and a matlab code based on Lagrange's interplanetary equations is developed. The effects of the atmospheric drag and the solar activity are investigated and the fuel and delta velocity consumptions are assessed for different deorbitation strategies. The paper also investigates the probability to hit or be hit by a piece of debris. A brief overview of the acquisition and safe hold modes *Bdot* and *Bspin* is given. Then the possibility to deorbit a satellite working in these attitude and orbit control modes from low Earth's orbits is studied. An attitude and orbit simulator is used to analyze the evolution of the attitude during a manoeuvre, in particular the effect of the thrusters' misalignment is investigated. A strategy which combines manoeuvres and aerobraking is chosen and its implementation on different types of orbits is studied. The paper concludes that the necessary manoeuvres for a 25 years deorbiting time can be achieve if the spacecraft has a functional acquisition and safe hold mode and an operational propulsion system. In the end an alternate mode based on star trackers and reaction wheels is developed to avoid most of the activations of the acquisition and safe hold mode and to eventually perform the end of life disposal of a spacecraft.

## Nomenclature

*Acronyms*

| | |
|---|---|
| LEO | Low earth's orbit |
| AOCS | Attitude and orbit control system |
| DV | Delta velocity |
| MJD | Modified julian date |
| BASS | Bi-axis sun sensor |
| MTQ | Magnetotorquer |
| EOL | End of life |
| NM | Normal mode |
| OCM | Orbit control manoeuvre |
| ASH | Acquisition and safe hold |
| FDIR | Failure detection and integrity recovery |
| RW | Reaction wheel |

*Parameters*

| | | |
|---|---|---|
| $r$ | Position vector | $[m]$ |
| $m$ | Mass | $[kg]$ |
| $\mu$ | Standard gravitational parameter (Earth) | $[km^3s^{-2}]$ |
| $S$ | Cross sectional area | $[m^2]$ |
| $\rho$ | Air density | $[kg/m^3]$ |
| $v$ | Velocity | $[m/s]$ |
| $r$ | Position vector | $[m]$ |
| $C_D$ | Drag coefficient | [1] |
| $a$ | Semi major axis | $[m]$ |
| $e$ | Eccentricity | [1] |
| $i$ | Inclination | $[rad]$ |
| $\omega$ | Advance of perigee | $[rad]$ |
| $\Omega$ | Regression of the node | $[rad]$ |
| $\nu$ | Actual orbit position | $[rad]$ |
| $J_j$ | Bessel coefficients | [1] |
| $\rho_p$ | Air density (perigee) | $[kg/m^3]$ |
| $H$ | Atmospheric scale height | [1] |
| $\omega_T$ | Earth's angular velocity | $[rad/s]$ |
| $\omega_{orb}$ | Orbit angular velocity | $[rad/s]$ |
| $\Omega_c$ | Control vector | $[rad/s]$ |
| $J_2$ | 0.001082 | [1] |
| $I_{sp}$ | Specific impulse | $[s]$ |
| $T$ | Torque | $[N*m]$ |
| $\Delta H$ | Change in angular momentum | $[N*m*s]$ |
| $B_{dl}$ | Lever of arm | $[m]$ |
| $M_{MTQ}$ | MagnetoTorQer | $[A*m^2]$ |
| $M_c$ | Commanded magnetic moment | $[A*m^2]$ |
| $F_{Tuy}$ | Thrusters | $[N]$ |
| $\Delta v$ | Delta velocity | $[m/s]$ |
| $\Delta t$ | Delta time | $[s]$ |
| $C_{mag}$ | Magnetic torque | $[N*m]$ |
| $A$ | Attitude matrix | [1] |
| $A_{opt}$ | Optimal matrix | [1] |
| $a_i$ | Weights | [1] |
| $r_i$ | Position in the inertial frame | $[m]$ |
| $b_i$ | Position in the spacecraft frame | $[m]$ |
| $B$ | Earth's magnetic field | $[Tesla]$ |
| $B_{meas}$ | $B$ measured | $[Tesla]$ |
| $\dot{B}$ | Earth's magnetic field derivative | $[Tesla/s]$ |

## Contents

# 1. Introduction

New regulations, applicable since January 2010, specify that all new satellites must be deorbited within 25 years. This is due to the progressive accumulations of orbiting debris. The orbital density of debris is now a threat for manned or unmanned missions and this law is a first step to keep the space environment safe. Most of the satellites launched since 1955 are now unpowered spacecraft wandering into space, and the great majority of debris are due to collisions, fuels tanks, rocket boosters etc. The strategies to deorbit satellites from LEO in case of system failure will be the main challenge of this project. Failures are likely to happen when a satellite reach its end of life and the deorbitation manoeuvres are difficult to implement in those cases. In case of system failure the satellite works in a very basic AOCS mode called "ASH". This study investigates possible mission scenarios to successfully deorbit spacecrafts from ASH modes. ASH modes considered here are based on the earth's magnetic field properties and they can be referred as magnetic modes. The attitude control system sensors and actuators are reduced to a minimum to ensure a minimum power level. Most of the time, the ASH mode only assures the angular rates reduction and the pointing of the normal to the solar arrays in the direction of the sun during daytime. A comparative study is done to choose the best strategic choice in term of mission safety and mission cost.

## A brief overview of the debris population

Figure 2 gives the density of objects per cubic kilometer; the curve is restricted to LEO. The object density is represented on a log scale and depends strongly on the altitude. Debris sizes superior to 1 cm can cause severe damage to a deorbitation mission so the corresponding object density is used in the computations. The orbital object density is calculated with the ORDEM2000 model of the NASA which gives reliable results. The debris population is studied by different agencies (ASI, BNSC, NASA, ESA, CNES, CNSA, DLR, ISRO, JAXA, NSAU, and ROSCOSMOS) and international regulations are decided by the Inter-Agency space Debris coordination Committee (IADC). In September 2007 IADC provided mitigation guidelines [1], the main measures are listed below.

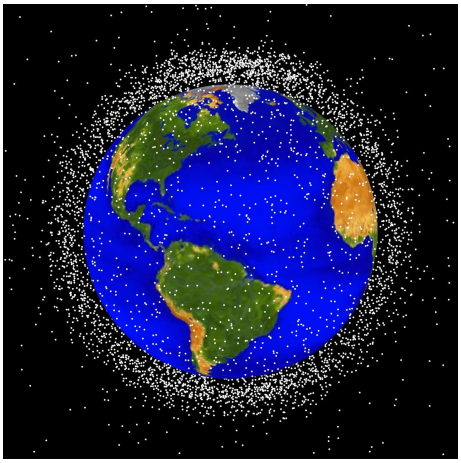

Figure 1: Debris Population (photo credit: NASA)

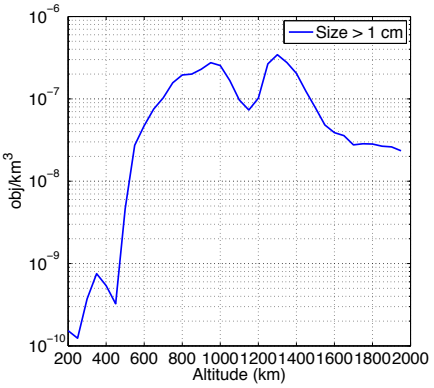


Figure 2: Debris Density

- Limit debris released during normal operations
- Minimize the potential On-Orbit Break-ups

- Equip all new satellites with post mission disposal systems

In [2] the NASA Orbital Debris Program demonstrates that there already exists altitude ranges where the concentration of debris will continue to grow even if a "no future launch" policy is applied. Therefore it is likely that international laws to mitigate the space debris population will become more strict and eventually companies which are not able to deorbit a spacecraft will have to pay extra fees. If the ability to perform a deorbitation mission from ASH modes is not granted the companies will have no choice but to deorbit the spacecraft after the first failure of one of equipment of the NM. The final purpose of this problem is to build a generic deorbiting mode and this study can be seen as a preliminary analysis, i.e. study the robustness of existing ASH modes during a standard deorbitation procedure.

### Typical AOCS modes

- The Normal Mode (NM) is used to perform the mission of the satellite. All the required performances are available in this mode
- The Orbit and Control Manoeuvre mode (OCM) is used to control the orbit, either to reach the operational orbit or to maintain the required orbital characteristics
- The Acquisition and Safe Hold mode (ASH) is used in case of system failure when an FDIR flag is raised the satellite switches to this mode. It is also used to damp the angular rates when the spacecraft is released from the launcher

## 2. Orbital mechanic analysis

An orbital mechanic analysis of the end of life phase is done to be able to assess the total deorbitation time. A matlab code is first developed and then validated. This code is then used to study different strategies to perform the deorbitation.

### 2.1. Model

Orbital perturbations can be of various types and will slightly affect the orbit so only the main ones will be implemented in the model. They are listed in Table I and their relative contribution on the orbit is assessed. The value of the solar pressure is valid in a LEO environment and the contribution of the aerodynamic forces is calculated at an altitude of 700 km.

| Perturbation | Acceleration |
|---|---|
| *Earth's Gravity* | 1 |
| *Aerodynamic forces* | $2 \cdot 10^{-8}$ |
| *Solar pressure* | $4.6 \cdot 10^{-7}$ |

Table I: Relative Acceleration due to the Space Environment

Although the magnitude of the solar pressure at high altitude is superior to the aerodynamic forces they will not be implemented in the model because they don't act in the opposite direction of the velocity vector. They will slightly drift the orbit during the deorbitation but at first order this is negligible. Therefore the satellite motion is given in Equation (1).

$$\ddot{\vec{r}} = -\frac{\mu}{r^3}\vec{r} - \frac{1}{2}\frac{C_D S}{m}\rho v \vec{v} \tag{1}$$

The drag force is modeled as in Equation (2).

$$D = \frac{1}{2} C_D \rho S v^2 \tag{2}$$

Equation (2) implies that a correct air density model must be used to assess a representative drag force during the mission scenario. The atmospheric model used is called MSIS-86. It depends on various parameters and particularly on the solar activity. As mission scenarios are likely to last 25 years, the influence of solar activity on the atmospheric density has to be taken into account. It is shown in a later section that this parameter has a great influence on the deorbitation time.

Equation (2) has been implemented in Simulink and gives accurate results but also extremely high computational times so an alternative model has been developed. It is based on the Lagrange's planetary equations which give the evolution of the orbital elements, this set of equations is given in [3]. It is also demonstrated in [3] that the variation of the semi major axis and the eccentricity over one revolution can be derived from the Lagrange's planetary equations. The solution is given in Equations (3) and (4). It is valid for an eccentricity inferior to 0.2 and only the gravity, the solar activity and the atmospheric drag are implemented in the model. Thus Equations (3) and (4) give the variation of the semi major axis and the eccentricity over one revolution. The alternative Matlab code uses theses equations to assess the deorbitation lifetime of a spacecraft.

$$\Delta a_{rev} = -2\pi\delta a^2 \rho_p \big(J_0 + 2eJ_1 + \frac{3}{4}e^2(J_0 + J_2) + \frac{e^3}{4}(3J_1 + J_3) + O(e^4)\big)e^{-c} \tag{3}$$

$$\Delta e_{rev} = -2\pi\delta a\rho_p\big(J_1 + \frac{e}{2}(J_0 + J_2) - \frac{e^2}{8}(5J_1 + J_3) - \frac{e^3}{16}(5J_0 + 4J_2 - J_4) + O(e^4)\big)e^{-c} \quad (4)$$

Where the following parameters have been used:

$$c = \frac{ae}{H}$$
$$\delta = \frac{QSC_D}{m}$$
$$n^2 = \frac{\mu}{a^3}$$
$$Q = 1 - \frac{2 \cdot \omega_T \cdot (1-e)^{3/2} cos(i)}{n\sqrt{1+e}}$$
$$J_j(c) = \frac{1}{2\pi}\int_0^{2\pi} cos(j\theta) exp^{c \cdot cos(\theta)} \cdot d\theta$$

Q is a factor which includes the rotation of the atmosphere.

The coefficients $J_j$ are the modified Bessel's functions of the first kind of order j, in all case they include the coefficient c.

## 2.2. Validation of the code

The matlab code based on Lagrange's interplanetary equations has been validated by a very accurate code called Matorb which is used at the orbital mechanics department at EADS Astrium. The results are presented in Figure 3. The accuracy lies within 5%. It is sufficient for this study but a larger number of simulations should be run to assess the accuracy of the code. In particular the influence of the eccentricity should be studied.

| Entity | Value | Units |
|---|---|---|
| $a$ | 6974.4 | $[km]$ |
| $e$ | 0.0153 | [1] |
| $i$ | 98.1886 | $[deg]$ |
| $MJD$ | 24838 | [1] |
| $S$ | 1.2 | $[m^2]$ |
| $m$ | 200 | $[kg]$ |
| $C_D$ | 2.3 | [1] |

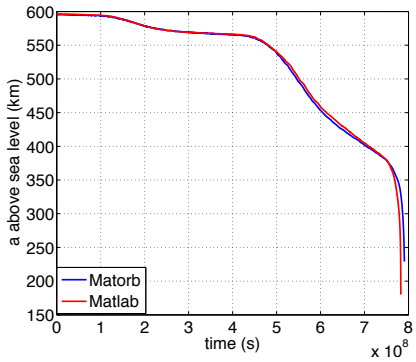


Figure 3: Comparison Matlab Code/ Matorb for a microsat configuration

## 2.3. Mission Scenario

Two scenarios are detailed to deorbit a spacecraft:

- Strategy 1 is based on an initial manoeuvre to change the perigee altitude. The perigee is moved to a lower region of the atmosphere where the air density is higher. The atmosphere is then used to brake the spacecraft, this phenomenon is called *airbraking* or *aerobraking*. It circularizes the orbit to an altitude where the drag force is sufficient to deorbit within 25 years. It is presented in Figure 4

- In Strategy 2, a device is used to increase the cross sectional area of the spacecraft. It increases the atmospheric drag and accelerates the reentry. Braking devices can be of various types (Air brake wing structure Figure 31, inflatable structure Figure 32, Tether, deployable membrane structure Figure 33, drag sails Figure 34)

Figure 4: Strategy 1

### 2.4. Reentry dynamics

Figure 5 gives a good overview of a spacecraft lifetime during its end of life mission. One can see that the initial altitude has a strong influence on the deorbitation time. It also depends on the ratio between the cross sectional surface and the mass of the satellite. The black dotted line represents a 25 years limit and for most of the satellites the ratio is around 0.005 therefore above approximately 600 km, a spacecraft in a circular orbit cannot deorbit itself naturally. As a consequence most of the satellites need an additional system or strategy to be deorbited within 25 years.

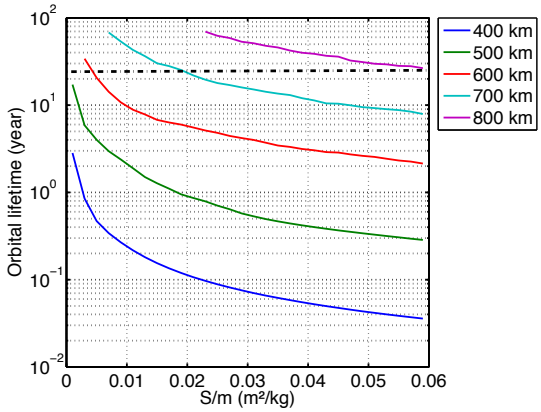


Figure 5: Orbital Debris Lifetimes

The following curves are given for the satellite THEOS [4], its characteristics are listed in Table II

| Entity | Value | Units |
|---|---|---|
| $a_{initial}$ | 7208 | $[km]$ |
| $e_{initial}$ | 0 | [1] |
| $i$ | 90 | $[deg]$ |
| $I_{sp}$ | 215.6 | [s] |
| $S$ | 4.76 | $[m^2]$ |
| $m$ | 673 | $[kg]$ |
| $C_D$ | 2.3 | [1] |

Table II: Simulation Imputs

### 2.4.1. Solar activity

The solar activity has an influence on the atmospheric drag because it affects the air density. Figure 6 shows this phenomenon. The parameter F10.7 represents the magnitude of the solar activity [5], a mean activity and a low. The corresponding evolutions of the semi major axis are plotted in the top part of Figure 6, a low solar activity can add few years to the mission time. Unfortunately it is not possible to have a reliable 25 years forecast of the solar activity.

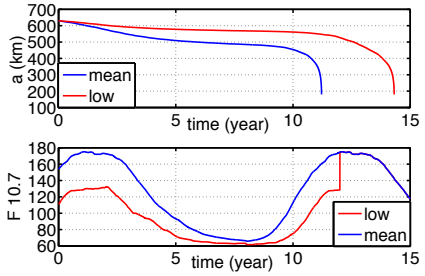


Figure 6: Influence of the solar activity on the reentry

Figure 7 shows that a small fuel quantity has a large impact on the deorbitation. Figure 8 implies that it doesn't cost a lot of fuel to prevent the mission from a low solar activity. THEOS has 77.1 kg of fuel for its total mission and 40 kg will remain in the end to perform the deorbitation manoeuvre so a low solar activity costs an additional 3.43 kg of fuel.

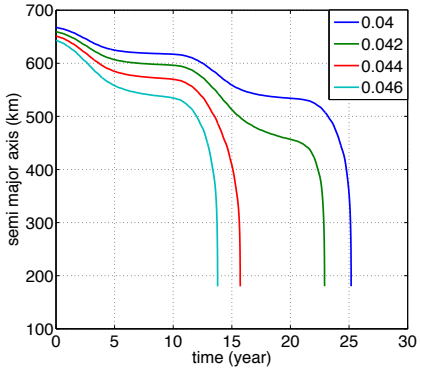


Figure 7: influence of a dedicated fuel quantity on the total mission time

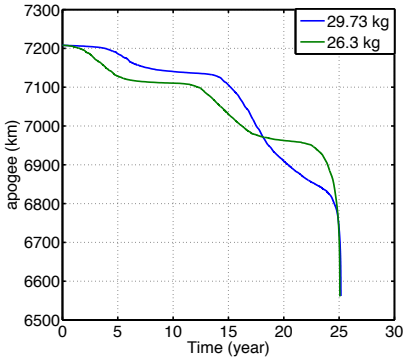


Figure 8: How to prevent a mission from a low solar activity

### 2.4.2. Orbital debris density

The risk of being hit by a piece of debris is assessed for the strategies 1 and 2. Figure 9 shows the evolution of the semi major axis during the end of life mission. It represents an approximation of the mean altitude over an orbit. On the same y-axis the debris population is plotted.The strategy 2 spends a great majority of its reentry in a high density region whereas the second one goes through relatively low object density. Moreover the cross sectional area has been increased a lot by the braking device, in the simulation the drag sail measures 30 square meter, this results in a much higher probability to hit a piece of debris during a mission based on strategy 2. Indeed Figure 10 shows how many orbital debris are hit since the beginning of each mission. The results shows 0.001 for strategy 1 and 0.073 for strategy 2. This is one of the drawback of strategy 2, it clearly increases the risk of being hit by an orbital object.

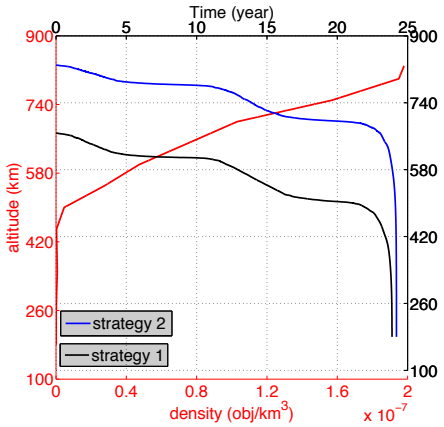


Figure 9: Collision with orbital debris

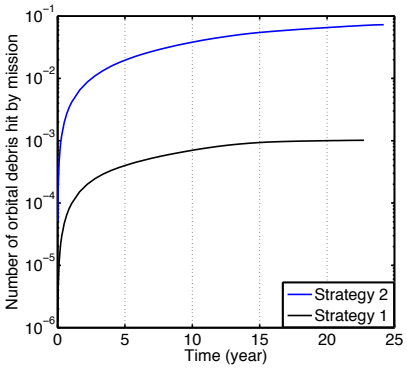


Figure 10: Probability to be hit by an orbiting object

### 2.4.3. DV manoeuvre

Strategy 1 starts with a DV manoeuvre to decrease the perigee to an altitude where the reentry can be done within 25 years. Figure 11 shows, for initial altitudes from 700 km to 1600 km, the corresponding DV. The type of manoeuvre depends on the propulsive strategy. The strategy called “Impulse” corresponds to only one impulse located at the North Pole in the opposite direction of the velocity vector. The other one, namely “Low

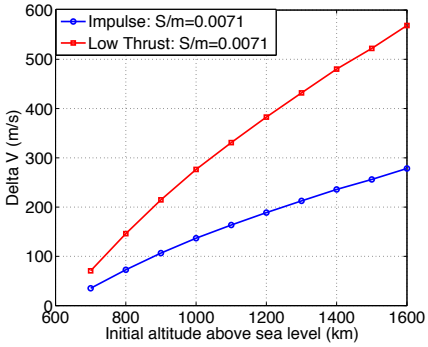


Figure 11: Delta V for a given scenario

Thrust", corresponds to a constant thrust force applied in the opposite direction of the velocity vector. Figure 11 shows that it is more effective to do only one impulse which makes sense because it only lowers the perigee rather than lower the entire orbit.

### 2.4.4. Drag sail analysis

The drag sail could be a solution to deorbit the spacecrafts. The main interest of the drag sails is that it involves passive technology, once the unfolding is done nothing else has to be done. Figure 12 gives the sail size as a function of the initial altitudes for initial masses between 200 kg and 700 kg to deorbit the spacecraft in 25 years. It has a strong non linear behavior therefore the utilization of sails to brake the spacecraft will be limited to low altitudes and low mass satellites. It is reasonable to limit the sail to 30 square meter because of the development cost and the operating risks.

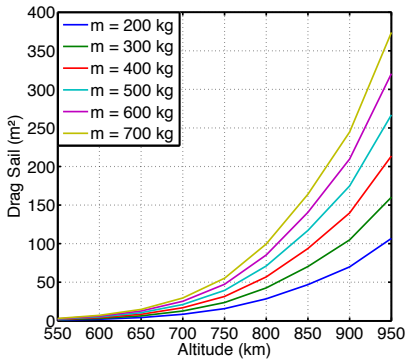


Figure 12: Estimated sail sizes to deorbit in 25 years

### 2.4.5. Electrodynamic tethers

An electrodynamic tether is a very long conductive tape which uses the earth's magnetic field via the Lorentz's force to brake a spacecraft.The pros and cons of using tethers is well studied in [8]. Even if electrodynamic tethers involve exiting technology, they will not be considered in the following study because they are not adapted to ASH modes. ASH modes are basic modes, i.e. only few sensors and actuators are still operational. The deployment of such tethers requires high precision sensors and actuators to avoid vibrations or structural failures and they are not available in ASH modes. Nevertheless

this technology presents some interests in terms of deorbitation times and mission cost and could be implemented in the NM but there are still many challenges to overcome.

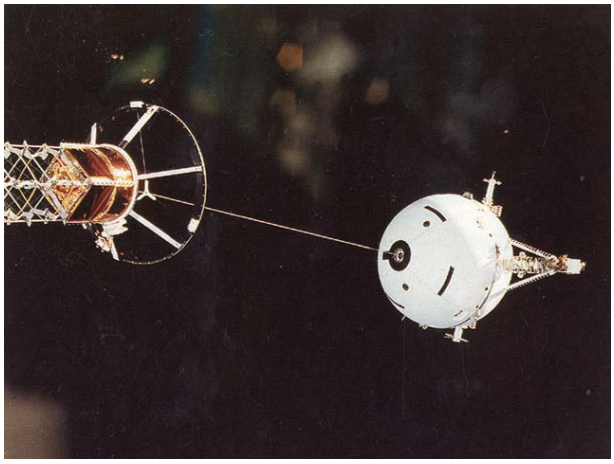

Figure 13: STS-46 Experiment, photo credit: NASA

To deorbit a spacecraft from LEO, electrodynamic tethers are typically 7-8 km long. Before they can be used as a potential strategy to mitigate the space debris population, two problems have to be investigated [8].

- To evaluate the impact of tethers on the space environment, i.e. to determine the tether collision risk with operating spacecraft, the risk posed by the tether remnants after severing, the chance of collision among the tethers themselves
- To assess the tether survivability, i.e. to evaluate the risk for a tether of being cut during the mission by orbital debris and micrometeorites

### 2.5. Discussion

Implementing a braking device to perform the deorbitation is very challenging. The system must deploy itself when the satellite reaches its end of life and in this case it must be able to do that in ASH modes. The system must not open itself when the satellite switches between normal and ASH mode it should work only if the satellite doesn't have the possibility to come back to NM. The risk to have system openings when it's not necessary must be considered and assessed because it simply means the total failure of the mission. Concerning the deployment of such a system it is also very challenging, avoiding structural modes for a tether for example. The system should also work without the need of any attitude control systems, i.e. to be aerodynamically stable or to have a cross sectional area independent of the satellite orientation. In [9] a system based on a dihedral aerobraking structure is presented and it respects the previous listed constraints but unintended openings are still likely to happen. It also means to carry the system as dead mass during the mission. For all of these reasons a strategy which uses propellant to perform manoeuvres is preferred when the fuel budget allows it. However there are configurations, especially micro satellite because they have a low surface to mass ratio, which require too much propellant to use a strategy only based on manoeuvres.

# 3. ASH Mode

This part is dedicated to the presentation of 2 ASH modes which are the most basic modes in a satellite, if these modes fail then the spacecraft is 'Lost In Space'. The possibility to deorbit a spacecraft from these modes will then be studied. This study is done to investigate a worst case scenario. Indeed it is very comfortable to be able to deorbit a satellite from one of these modes because even in a scenario where the satellite is locked in a ASH mode it is still possible to perform the deorbitation.

### Axis convention

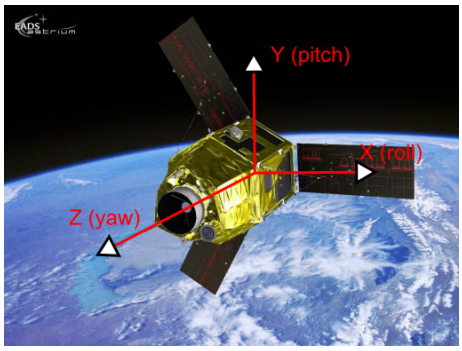


Figure 14: Axis convention, photo credit: Eads Astrium

## 3.1. Bdot

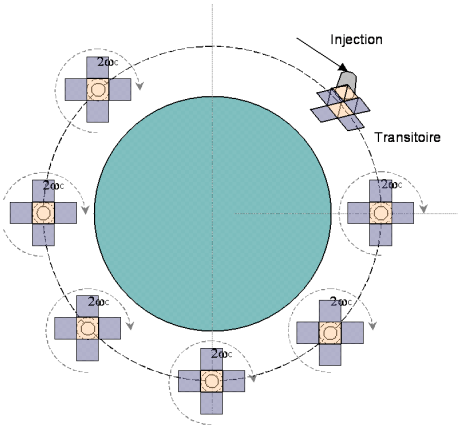


Figure 15: Bdot

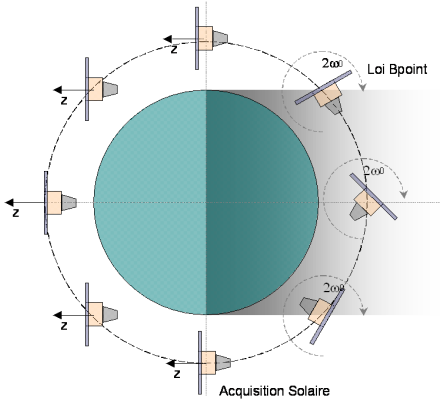


Figure 16: Bdot law + solar acquisition for a noon-midnight orbit

The $B_{dot}$ law uses the properties of the Earth's magnetic field to apply a torque to the satellite. This torque is designed to be applied in the direction opposite to the local variation of the magnetic field in the spacecraft frame. Its expression is given in Equation (5). For large angular rates the Earth's magnetic field is assumed to be locally constant in the inertial frame therefore Equation (5) tends to reduce angular rate.

$$\vec{T} = (-k\dot{\vec{B}}) \times \vec{B} \tag{5}$$

Magnetometers are used to estimate $B_{Rsat}$ and then magnetorquers are used to generate the magnetic moment $-k\dot{B}$. Document [11] shows that this law dissipates energy. The

converged state corresponds to the satellite following the magnetic field streamlines, i.e. orbiting at twice the orbital angular velocity. Without any onboard angular momentum the satellite rotates around the axis with the largest inertia and this axis is aligned with the normal to the orbit. Figure 15 represents the typical motion of a spacecraft in the $B_{dot}$ mode. However in order to respect the power budget a reaction wheel is added to the system to perform the pointing of the solar array during daytime. It simply blocks the pitch axis to minimize the output of the sun sensor. A detailed presentation of this magnetic mode can be found in [6]. This motion is sketched in Figure 16.

### 3.2. Bspin

The Bspin concept is similar to the Bdot law, the main difference lies in the gyroscopic stiffness creation. Indeed in the Bdot law the gyroscopic stiffness is created by a reaction wheel whereas for the Bspin law the satellite is spun to produce gyroscopic rigidity. This ASH mode works with very few sensors and actuators (magnetometers, MTQ and BASS), moreover these equipments are very reliable. As a consequence the Bspin mode has a very low probability to fail. The typical Bspin motion is described by 17, as one can see the spacecraft is spinning around one of his principal axis of inertia and it aligns this axis with the normal to the orbit. Many satellites are on sun synchronous orbit with local time close to 10h/22h, this orbit is sketched in Figure 23. To have a maximum efficiency of the solar generator the spin axis must be aligned with the normal to the solar array and it has to point in the direction of the sun. As described in Figure 18 it is possible to do that with the Bspin law. An axis reorientation law is added to the Bspin law in order to perform this manoeuvre, it uses only the available sensors and actuators, therefore it does not increase the probability of failures for the Bspin mode.

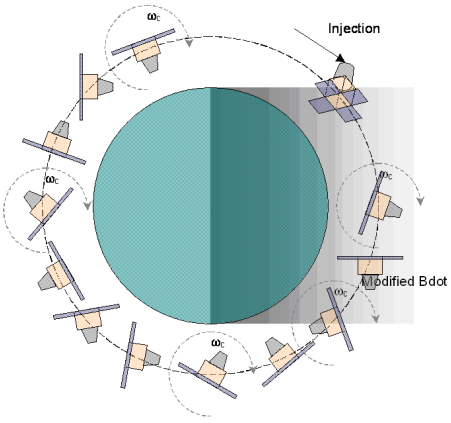


Figure 17: Typical Bspin motion on a noon/midnight orbit

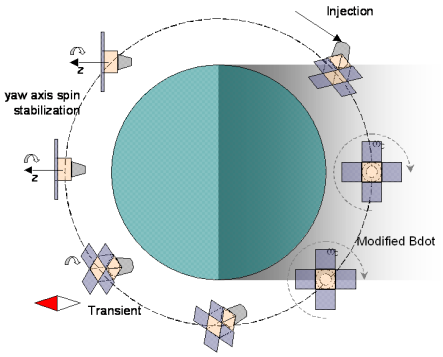


Figure 18: Synoptic of the Bspin law with reorientation of the spin axis

The Bspin Law is given in Equation (6), $M_c$ is the command which is sent to the MTQ. The corresponding torque is produced by interaction with the earth's magnetic field as written in Equation (7).
The abbreviation *proj* is the projection on the plane normal to the instantaneous direction of the measured magnetic field. In the problem case described in Figure 17 the control vector $\Omega_c$ is chosen to be aligned with the pitch axis therefore the illumination of the solar array happens half of the time during daytime. The converge state corresponds to the satellite spinning at $\big((2+\alpha)\omega_{orb}\big)$ around the chosen axis with this axis aligned with the normal to the orbit.

$$M_c = proj\big( - k(\dot{\vec{B}}_{meas} - \vec{\Omega_c} \times \vec{B}_{meas})\big) \tag{6}$$

$$\vec{T} = \vec{M_c} \times \vec{B} \tag{7}$$

$$\vec{\Omega_c} = \big[0, \alpha\omega_{orb}, 0\big] \tag{8}$$

In an ideal case it would be better to have the satellite strictly pointing the sun to maximize the illumination, it is represented in Figure 18. An axis reorientation control law has been added in Figure 18, it uses the data from the BASS to orient the spin axis in the direction of the sun. This law is described in [10].

## 4. Deorbitation from ASH modes

The implementation of strategy 1 in ASH modes is derived in this section. The analysis is focused on how to point the thrust vector in a optimal direction to perform a manoeuvre and what are the effect of the manoeuvre on the spacecraft attitude.

### 4.1. Evolution of the attitude during the manoeuvres

#### 4.1.1. Misalignments of the thrusters

The magnetic control laws suffer from an angular momentum perturbation when a DV is done. In the OCM mode the thrusters are tuned in order to produce a minimum total torque during a commanded manoeuvre. They are adjusted by setting the off modulation coefficients of the thrusters to an optimal value. However it is not possible in ASH modes due to the lack of sensors and actuators therefore there is a residual torque produced by the thrusters' misalignments. This angular momentum perturbation is given by Equation (13). The magnetic laws are very slow to damp such a perturbation which is a problem because the ASH modes must stay in a converged state to assure the illumination of the solar arrays so the destabilization induced by the manoeuvre has to be damped quickly.

$$\Delta H = B_{dl} \cdot m \cdot \Delta v \tag{9}$$

$$C_{mag} = M_{MTQ} \cdot B \tag{10}$$

$$\Delta t = \frac{B_{dl} \cdot m \cdot \Delta v}{M_{MTQ} \cdot B} \tag{11}$$

$$\Delta v = \frac{M_{MTQ} \cdot B \cdot \Delta t}{B_{dl} \cdot m} \tag{12}$$

$$\Delta H = F_{tuy} \cdot \Delta t \cdot B_{dl} \tag{13}$$

Figure 19 shows what happen to $Z_{sat}$ in the inertial space, $X_i$ represents the direction of the sun and the ideal steady state of the system is $Z_{sat}$ aligned with $-X_i$. From the preliminary analysis it has been shown that for satellites in the same mass and inertia range as THEOS the $B_{dot}$ mode can withstand an angular momentum perturbation of 5 $Nms$ . Depending on the lever of arm of the thrusters it can strongly limit the maximum delta V ( $\approx$1 m/s ) for one impulse. This can result in a large number of manoeuvres and so in large ground operation times.

To limit this effect the data from the BASS can be used to manually change the off modulation coefficients of the thrusters in order to reduce the size of patterns in Figures 20 and 21. Figures 20 and 21 shows the BASS data during the DV manoeuvre. The tuning step by step of the off modulation coefficients produce the black patterns instead of the green one so it shows an amelioration of the total torque.

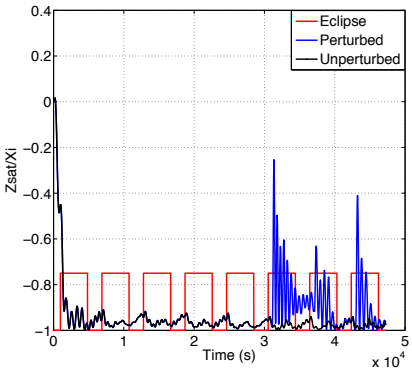


Figure 19: Effect of the thrusters' misalignments

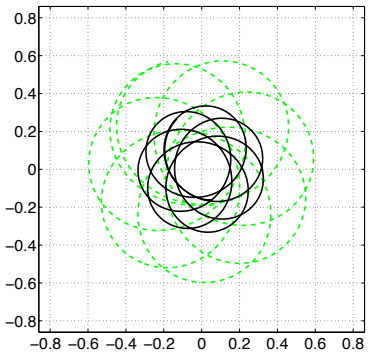

Figure 20: Sun sensor DATA, free dynamics

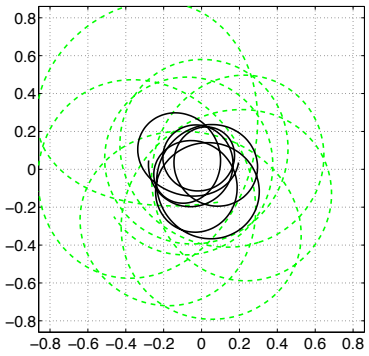

Figure 21: Sun sensor DATA, Bspin control

### 4.1.2. Correction of thrusters' misalignments

It has been shown that the thrusters' misalignments can be reduced step by step. This method induces large ground operation time and cannot be reasonably implemented. Two situations can arise:

- The satellite is working in NM, an unpredictable event happens and this results in a total loss of the NM. In this case the last value of the off modulation data are used as a basis to adjust the thrusters
- The satellite has never been able to work in NM so the ground test data of off modulation are used to begin the deorbitation

## 4.2. Pointing of the thrust vector in ASH modes

The ASH modes are designed to point in the direction of the sun during day time so the best position to perform the manoeuvre will be at the Poles. Figure 22 shows the successive manoeuvres which start the deorbitation strategy, the total number of impulses depends on:

- The capacity of the thrusters
- The efficiency of the impulses (if the thrust vector and the velocity vector are well aligned)

- The maximum amount of angular momentum that can be added to the magnetic mode during one impulse. It is directly related to the thrusters' misalignments and the order of magnitude lies between 1 $Nms$ and 10 $Nms$ for a satellite like THEOS. This limitation must be guaranteed otherwise the pointing of the solar arrays will not be sufficient to respect the power budget and the spacecraft will run out of energy

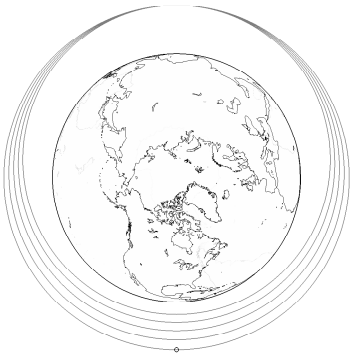

Figure 22: Strategy

### 4.2.1. Sun synchronous orbit

The $B_{dot}$ mode is aligned with the velocity vector at the Poles whereas the $B_{spin}$ is aligned with the direction of the sun. On a sun synchronous orbit with a local hour different from 12/24h the direction of the sun and the direction of the velocity vector makes a non zero angle. Figure 23 presents this situation on a 10/22h orbit, in this case the angle is equal to 30°. We assume that the main direction of the propulsive system is the same as the direction of the velocity vector. In $B_{spin}$ the manoeuvre will be done in the direction of the sun instead of in the direction of the velocity vector. As a consequence the fuel quantity to perform the manoeuvre will be increased by 15.4 %. A Simulink model has been developed to check this theoretical result, a screen-shot of the simulator is given in Figure 30.

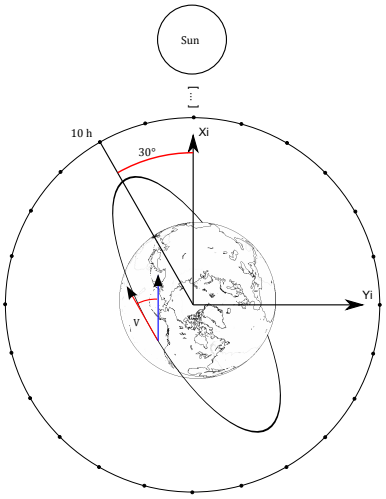


Figure 23: Bspin with axis reorientation facing a non optimal pointing of the thrust vector during an impulsive manoeuvre

| Entity | Value | Unit |
|---|---|---|
| $a$ | 7208.1 | $[km]$ |
| $e$ | 0 | [1] |
| $i$ | 98.8 | $[deg]$ |
| *initial date* | 20/04/2010 | [1] |
| $S$ | 4.76 | $[m^2]$ |
| $m$ | 672.3 | $[kg]$ |
| $C_x$ | 2.3 | [1] |
| $\Omega$ | -30 | $[deg]$ |
| $\omega$ | 0 | $[deg]$ |
| $\nu$ | 0 | $[deg]$ |

Table III: Initial conditions

The simulation is done with the following asumptions and the initial conditions are written in Table III :

- The impulses are done in the direction of the sun (Xi=[1 0 0]) every orbit and each of them corresponds to a $\Delta V$ equal to 1 m/s

The Simulink model gives a total $\Delta V$ equal to 95 m/s and the theory also gives 95 m/s. If the angle between both directions is 0° instead of 30° the total $\Delta V$ is 82.3 m/s. There is an increase by 15.4 % of the fuel quantity which corresponds to 4 kg more for THEOS. This is problematic and it could lead to a modification of the current magnetic modes. This problem is specific to the Bspin mode because it strictly point in the direction of the sun. The Bdot mode doesn't have this drawback because it locks the pitch axis to point the sun to be aligned with the projection of the sun direction on the orbit plane.

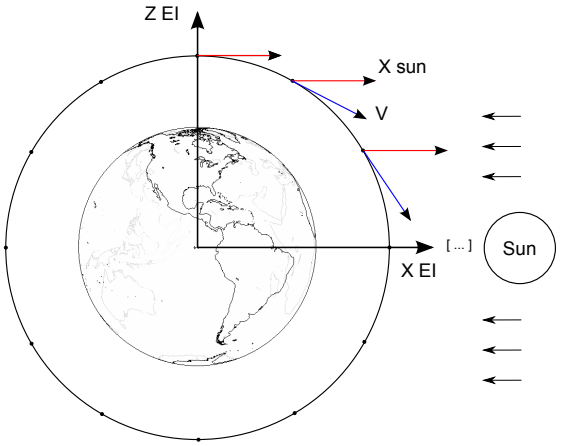


Figure 24: Bdot with axis reorientation facing a non optimal pointing of the thrust vector during an impulsive manoeuvre

However there is another problem which is present both in the Bspin and the Bdot mode. The problem case is sketched in Figure 24. 80 m/s is a common value to deorbit a spacecraft from LEO, obviously this cannot be done in 1 impulse in the ASH mode but even an impulse corresponding to 3 m/s take some time to be done and as sketched the velocity vector and thrust vector are only aligned above the North Pole. If the impulse is too long the misalignment affects the total $\Delta V$ so the fuel quantity dedicated to deorbit the spacecraft increases.

### 4.2.2. Drifting orbit

Prograde or retrograde orbits can face a different problem which is shown in Figure 25. The velocity vector and the direction of the sun are aligned twice a year which increases the ground operation times. A solution can be to change the target value in the axis reorientation control loop system. A solution is explained in the next subsection.

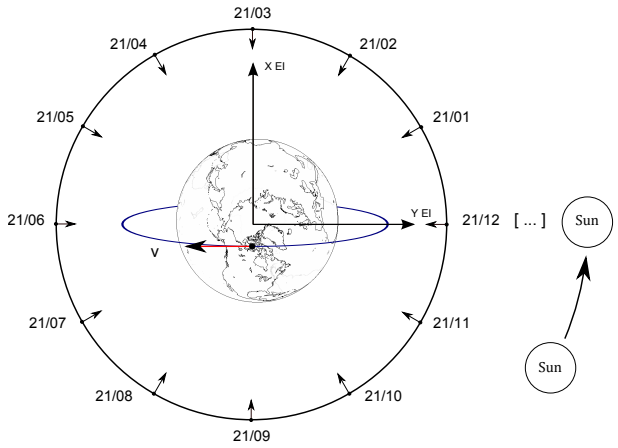


Figure 25: Satellites in prograde or retrograde orbits facing a phasing problem to align the velocity vector at North Pole with the direction of the Sun

### 4.2.3. Attitude determination from BASS and magnetometer data

Only a BASS and 3 magnetometers are available in Bspin, therefore two directions can theoretically be observed in the spacecraft frame, namely the direction of the sun and the direction of the earth's magnetic field. Both directions can also be assessed in the earth's inertial frame so it is possible to estimate the quaternion from the inertial frame to the spacecraft frame. The method is described in [7]. The three axis attitude determination problem is posed in term of finding the optimal matrix $A_{opt}$ which minimizes the problem presented in Equation (14). This function is a least squares loss function and the corresponding problem can be solved by a method described in [7] which involves the singular value decomposition of the matrix B given in Equation (15).

$$L(A) = \frac{1}{2}\sum_{i=1}^{n} a_i |b_i - Ar_i|^2 \tag{14}$$

$$B = \sum_{i=1}^{n} a_i b_i r_i^T = USV^T \tag{15}$$

This solution is also known as the SVD solution to Wahba's problem. Finally the optimal matrix $A_{opt}$ is given by Equation (16). The parameter $d$ is the product between the determinant of $U$ and the determinant of $V$ and can be equal to 1 or $-1$.

$$A_{opt} = U[diag(1, 1, d)]V^T \tag{16}$$

$A_{opt}$ is the direction cosine matrix from the inertial frame to the spacecraft frame and can easily be transformed into the corresponding quaternion and be used in the Simulink computations.

### 4.2.4. An alternative to change the pointing of the Bspin mode

The theory explained in the previous part is applied here. Two directions are used in the algorithm, namely the direction of the earth's magnetic field and the direction of the sun. The problem is the one described in Figure 23 and the magnetic mode used is the Bspin mode. As explained before the target direction in the axis reorientation control law has

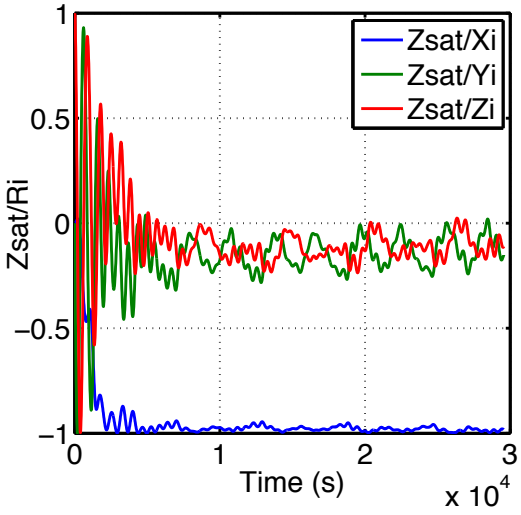


Figure 26: Normal

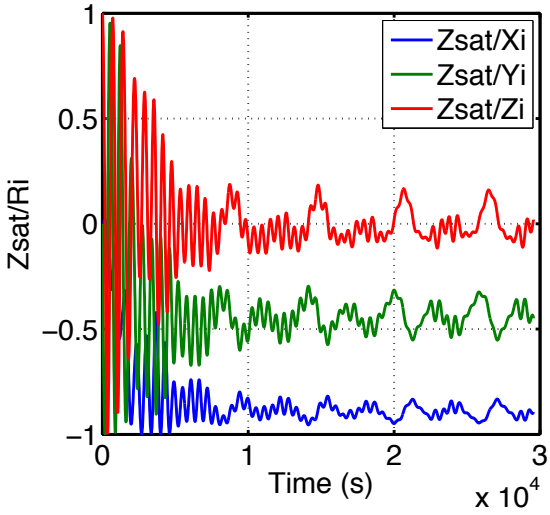


Figure 27: Biased

to be changed to point in the direction of the velocity vector at the North Pole. Figure 26 shows the coordinate of $Z_{sat}$ in the inertial frame in a normal case whereas Figure 27 shows what happens when the theory described in the previous subsection is applied. The orbit plane and the direction of the sun makes a 30° angle so the direction of the velocity vector at the Poles should be $[+/-cos(\pi/6), +/-sin(\pi/6), 0]$. In Figure 27 the coordinates are close to $[-cos(\pi/6), -sin(\pi/6), 0]$ so it works and it's worth doing a more detailed analysis, for example adding instrumental noises to the sensors and actuators.

## 4.3. Ground operations

It is interesting to plan a semi automatic strategy to have a limited number of people who work on the deorbitation. It could be interesting to plan the manoeuvres for one day then to check if they have been well executed and to modify the off modulation coefficients to optimize the thrust vector. The deorbitation is done at the North Pole or at the South Pole so the field of view of polar satellite tracking stations has to be investigated to check if the data can be transmitted all the time. Figure 28 shows the field of view of satellite tracking stations near the Poles for a sun synchronous orbit at an altitude of 800 km. The black dotted lines at the top and at the bottom in Figure 28 represent a region of $+/-23°$, depending on the season it represents the inclination between the sun direction and the equatorial plane. It simply means that the coordinates where the velocity vector and the direction of the sun are aligned depends on the date. Those two zones are limits, the coordinate of the manoeuvre will always lies in these zones. The red curve is the ground trace of the satellite, this graph shows that the satellite can be seen by satellite tracking stations. Namely those stations are, Svalbard (Norway), Kiruna (Sweden), Kerguelen (Kerguelen Islands), Troll (Antartic). A more detailed analysis should be done to determine if a semi-automatic strategy can be implemented but at least it is possible to send commands to the satellite to perform the manoeuvres.

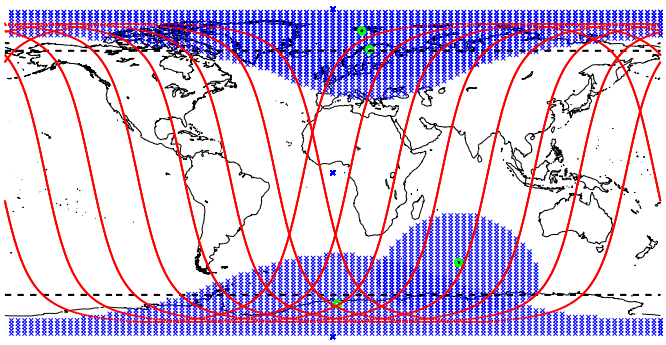

Figure 28: Field of view of TM/TC tracking stations corresponding to a 800 km circular sun synchronous orbit

### 4.4. Discussion

We can reasonably expect to achieve the necessary manoeuvres for a 25 years deorbiting time if:

- We have a functional propulsion system
- The ASH mode is operational

This allows to avoid oversizing the redundancy architecture of the NM equipments for meeting the requirements of the new 25 years rule. Moreover we can reasonably expect that the deorbiting manoeuvres will be conducted with the NM hardware most of the time. We can also expect that even if the NM is dead due to a failure on an essential equipment of this mode there are still most of the sensors and actuators of the NM which are still functional.
The end of life disposal of a satellite is difficult to implement when the satellite is driven by a magnetic control law and an intermediate mode between the NM and the ASH mode would be of great help to perform the required manoeuvres. It's more comfortable to deorbit a satellite if the mode is based on star trackers and reaction wheels rather than on magnetometers, magneto torquers and a solar sensor. However this mode should not represent a risk to be 'Lost In Space' so it should have a short convergence time in comparison to the ASH mode because if it fails then the ASH mode must have the time to converge. ASH modes usually converge in 3 to 4 orbits therefore this mode should have a short time out in comparison. Moreover it should not lead to conditions where the ASH mode cannot converge so it must avoid the creation of very high angular rates ($3°/s$). It can also be used to have a fast recovery from a ASH state, for example the satellite starts converging in the ASH mode to reduce angular rates and once the total angular momentum of the satellite lies in the envelope of the reaction wheels, it switches to this alternate mode to finish the rate reduction and to perform the pointing of the satellite. Moreover it can also avoid most of the activations of the ASH mode, for example an FDIR flag appears, instead of going directly to the ASH mode the satellite starts this

alternate mode. This mode will be designed to converge quickly so if it works the ASH mode doesn't need to be activated and if it fails it doesn't compromise the convergence of the ASH mode.

## 5. Conclusion

In this study an orbital mechanic analysis of the deorbitation has been presented and implemented in a matlab code to estimate the deorbitation lifetime with low computational time and good accuracy. This code has been validated by a more accurate code. An overview of two ASH modes used at Eads Astrium has been made as an introduction to an analysis of satellite deorbitation strategy from ASH modes. The implementation of a strategy based on manoeuvres and aerobraking has been conducted. Depending on the orbit and on the type of ASH mode a non negligible quantity of fuel is wasted, this is due to a non optimal pointing of the ASH mode and to the misalignments of the thrusters. This strategy involves high ground operation times because the ASH mode can only withstand a small impulse each orbit. A solution based on an attitude determination algorithm using vector observations and the singular value decomposition is presented to reduce the amont of fuel required to deorbit a spacecraft in ASH mode. The implementation in Simulink shows encouraging results. As a consequence we can reasonably expect to achieve the necessary manoeuvres for a 25 years deorbiting time if we have a functional ASH mode and an operational propulsion system.

## 6. Acknowledgments

I am very grateful to my thesis supervisors, Kristen Lagadec and Claire Roche, for all their ideas and advices which always helped me during this project. I also want to thank Slim Locoche, Anne-Helene Gicquel and David Joalland for their help in orbital mechanics. Besides, I am thankful to all the advanced studies department at EADS Astrium which provided me a good working environment and good facilities to complete this project. It was a pleasure to work here for 6 months.

Lastly I would like to express my deepest sense of gratitude to my supervisor at KTH, Professor Dan Borglund, for his teaching at KTH which impressed me in numerous ways, and for reviewing my thesis report.

## References


[1] IADC: *IADC Space Debris Mitigation Guidelines* , 2007

[2] Orbital Debris Quarterly News, NASA, Volume 14, issue 1, January 2010

[3] David Anthony Vallado: *Fundamentals of Astrodynamics and Applications*, Wayne D McClain, 2001

[4] Wikipedia: $http://en.wikipedia.org/wiki/THEOS_(satellite)$, 2010

[5] NASA website: $http://solarscience.msfc.nasa.gov/predict.shtml$, 2010

[6] P. LAURENS: *Quelques reflexions sur un mode normal et d'acquisition gyroless pour un microsatellite LEO*, EAA.NT.PhL.4774.99, 1999

[7] F. Landis Markley: *Attitude determination using vector observations and the singular value decomposition*, NASA, 1988

[8] C. Pardini, T. Hanada, P. H. Krisko: *Benefits and risks of using electrodynamic tethers to deorbit spacecraft*, IADC, IAC-06-B6.2.10

[9] Vincent Peypoudat, Olivier Le Couls: *Satellite Air Brake Wing Structure*, Patents, International Publication Number, WO 2007/096289A1

[10] Kristen LAGADEC: *Loi Bspin : modes d'acquisition et survie sans actionneurs inertiels*, ASG64, EAA.NT.KL.XXXX.00, 2000

[11] Celine BEUGNON: *Overview of a magnetic safe mode*, ASG64, DIV.TCN.00022.T.ASTR, 2006

[12] Dana G. Andrews: *Aerodynamic braking system for a space vehicle*, patents, US4518137, The Boeing Company, 1985

[13] Kerry T.Nock, Angus D. McRonald, Kim Maynard Aaron: *Balloon device for lowering space object orbits*, patents, US6,830,222 B1, Global Aerospace Corporation, 2004

[14] Harkness, Patrick George: *An aerostable drag-sail device for the deorbit and disposal of subtonne, low earth orbit spacecraft*, Phd Thesis, Cranfield University, 2006

# 7. Annexe

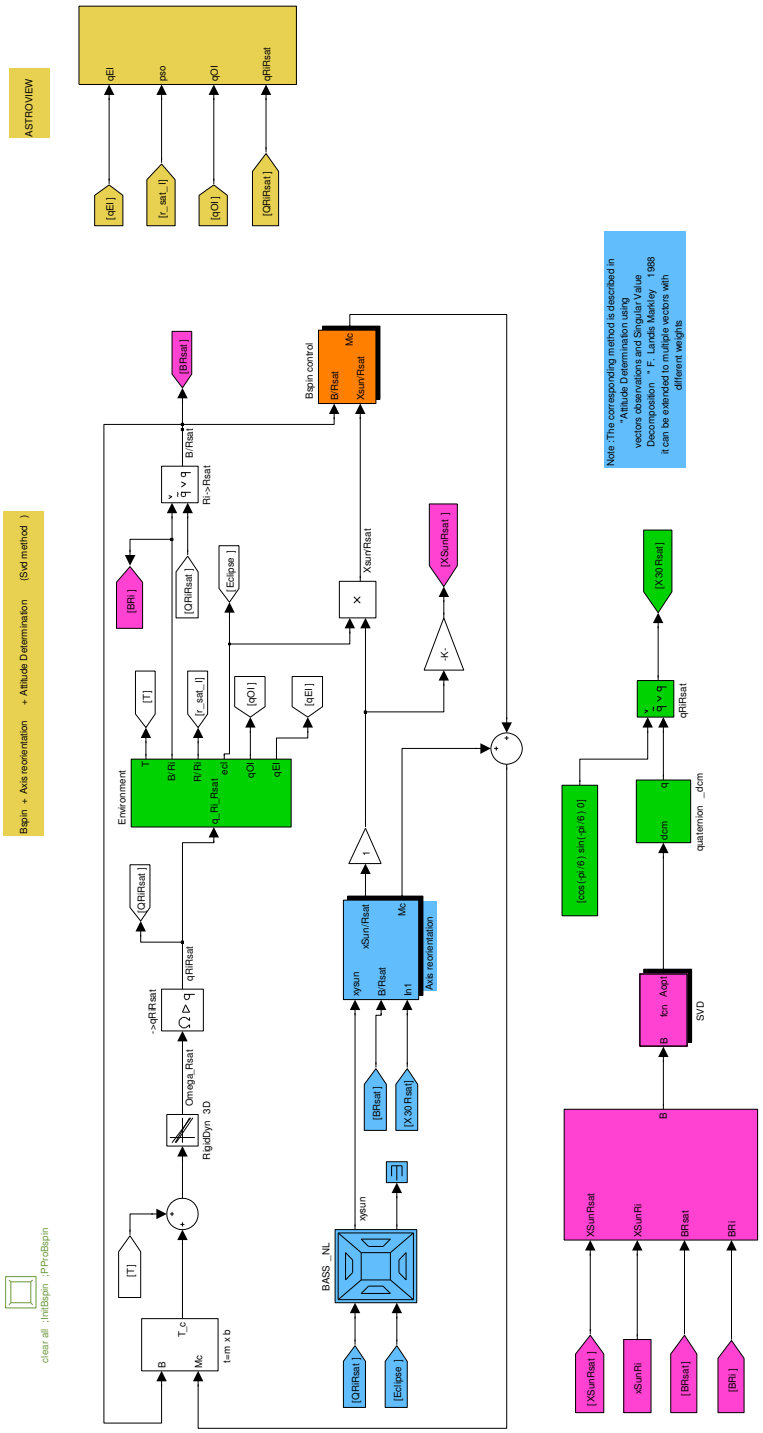


Figure 29: Attitude and Orbit Control Simulator

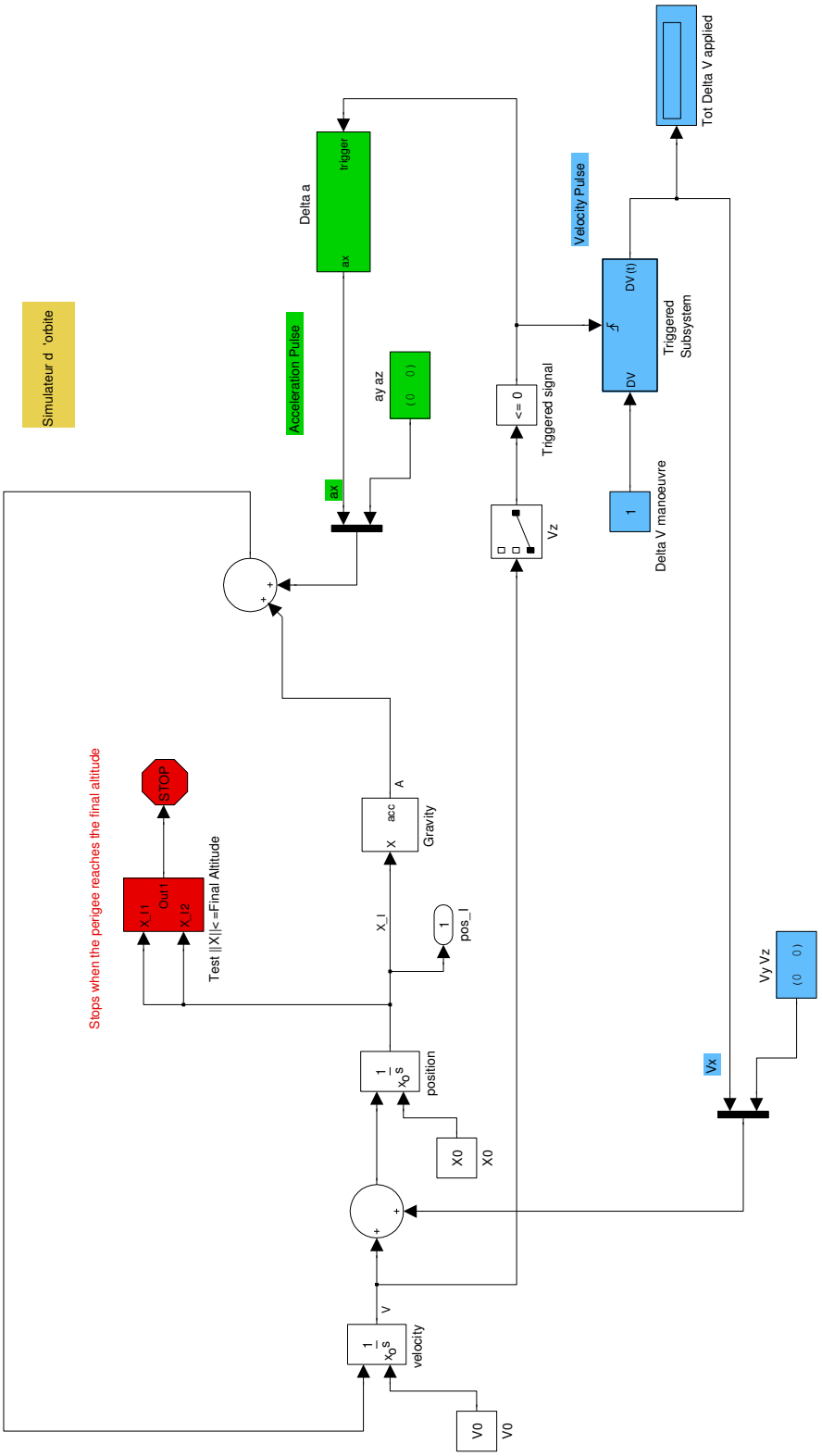


Figure 30: Orbit Simulator

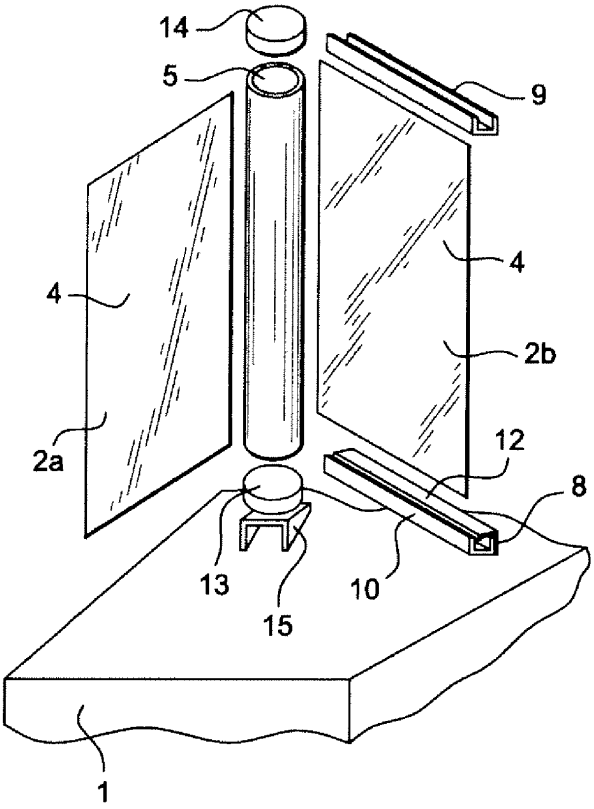


Figure 31: Dihedral airbrake wing structure, photo credit: [9]

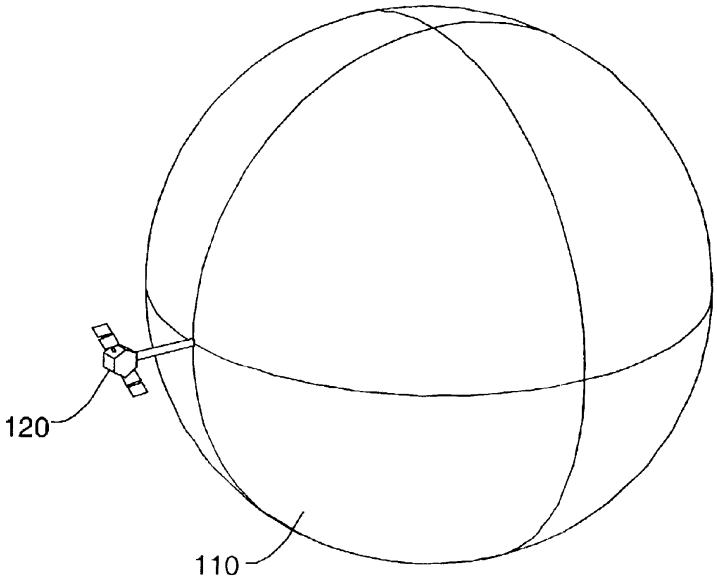


Figure 32: Braking balloon, photo credit: [13]

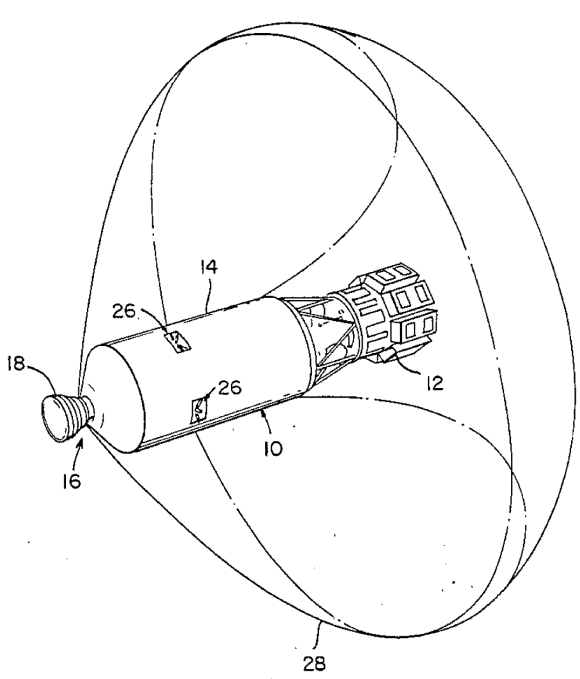


Figure 33: Braking membrane, photo credit: [12]

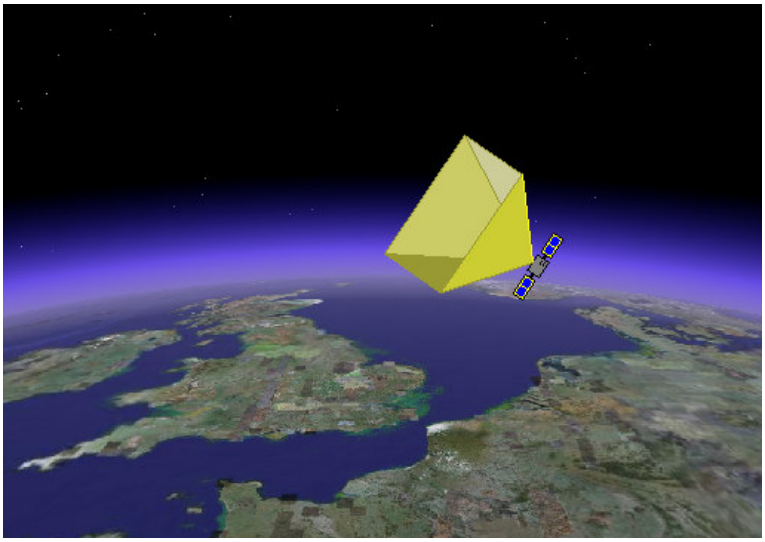

Figure 34: Aerostable drag sail, photo credit: [14]

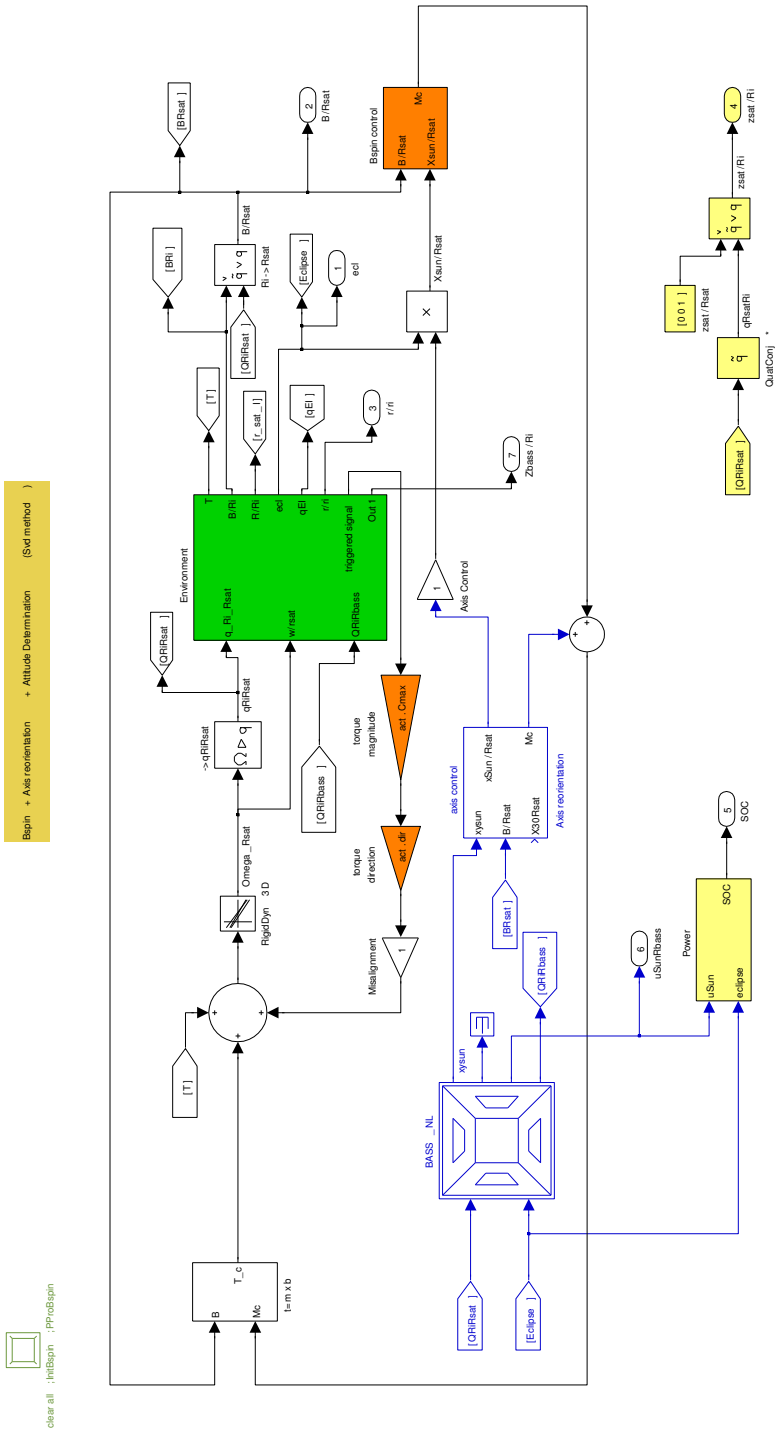


Figure 35: Orbit Simulator and AOC simulator